Electrochimica Acta 56 (2011) 3159–3163

Contents lists available at ScienceDirect

Electrochimica Acta

journal homepage: www.elsevier.com/locate/electacta

Porphyrin-functionalized gold nanoparticles for selective electrochemical detection of peroxyacetic acid

Jie Li, Wenwen Tu, Jianping Lei*, Sheng Tang, Huangxian Ju*

Key Laboratory of Analytical Chemistry for Life Science (Ministry of Education of China), Department of Chemistry, Nanjing University, Nanjing 210093, PR China

ARTICLE INFO

Article history:
Received 20 October 2010
Received in revised form
27 December 2010
Accepted 4 January 2011
Available online 22 January 2011

Keywords:
Porphyrin
Electrocatalysis
Gold nanoparticles
Layer-by-layer assembly
Peroxyacetic acid

ABSTRACT

Two layers of cationic iron(III) meso-tetrakis (N-methylpyridinum-4-yl)porphyrin (FeTMPyP) and anionic gold nanoparticles (GNPs) were alternately assembled on a poly(diallyldimethylammonium chloride)-wrapped carbon nanotube (PDDA-CNT)-modified electrode via electrostatic interactions. The porphyrin-functionalized gold nanoparticles were characterized by scanning electron microscopy and UV–vis absorption spectrometry. The $(FeTMPyP–GNP)_2$/PDDA-CNT modified electrode showed two stable and well-defined peaks at −0.112 V and −0.154 V, which were attributed to the GNP-accelerated redox process of Fe(III)TMPyP/Fe(II)TMPyP. The modified electrode possessed excellent electrocatalytic behavior for the reduction of peroxyacetic acid (PAA). The resulting biosensor exhibited a fast amperometric response to PAA (~3 s), with a wide linear range from 2.5×10^{-6} M to 1.05×10^{-3} M and a detection limit of 0.5 μM at a signal-to-noise ratio of 3. More importantly, H_2O_2 did not interfere with the detection. Thus, this biosensor enabled highly sensitive detection of PAA without removing H_2O_2 and showed a promising potential in practical applications.

1. Introduction

Peroxyacetic acid (PAA) is widely used in the food and cleaning industries as an ideal disinfectant [1], as its strong oxidizing power can rapidly kill all microorganisms such as viruses, bacteria, fungi, and spores. However, a high concentration of PAA may cause skin and mucosal irritation in humans and even cause burns. Thus, there exists a need for a quick and easy method for the detection of PAA. Several methods have been developed for PAA detection, such as titration [2], photometry [3], spectroscopy [4], and gas or liquid chromatography [5–8]. Although these methods have adequate sensitivity, they often suffer from the need for time-consuming derivatization and extraction steps. To make use of the advantages of electrochemical analysis, Ohsaka and coworkers [9] developed a novel electroanalytical method for PAA detection in the presence of H_2O_2 using a rotating gold-disk electrode. Bontempelli and coworkers [10] then used a rotating Pt- or gold-disk electrode to further study the electrochemical behaviors of PAA and H_2O_2 and achieved the selective detection of PAA and H_2O_2 in cosolution. However, rotating disk electrodes are obviously difficult to use for *in situ* or online monitoring. Thus, it is of interest to seek an efficient catalyst for the selective detection of PAA.

Porphyrins are an important class of conjugated organic molecules and have been employed to mimic the active sites of many important enzymes, such as hemoglobin, myoglobin, cytochrome *c* oxidase [11], nitric oxide reductase [12], vitamin B_{12} [13], and chlorophyll [14]. The metalloporphyrins, especially iron porphyrins, can be used as electronic media based on their reversible Fe(III)/Fe(II) redox states and exhibit good electrocatalysis for biologically important molecules [15–19], including dissolved oxygen [15,16], NO [17–19], and nitrite [12]. Thus, we studied the electrocatalytic activity of iron(III) meso-tetrakis (N-methylpyridinum-4-yl)porphyrin (FeTMPyP) for the reduction of PAA and H_2O_2 by assembling alternate layers of FeTMPyP and gold nanoparticles (GNPs) on a poly(diallyldimethylammonium chloride)-wrapped carbon nanotube (PDDA-CNT)-modified electrode.

Porphyrin-functionalized nanoparticles are expected to have significantly different chemical activities from those of free porphyrins [20–23]. The controlled organization of functional porphyrins into highly ordered nanomaterials has showed great potential in photoelectrochemical applications by improving the photoelectrochemical transfer efficiency [24–29]. Furthermore, their application to electrochemical biosensing has attracted considerable attention. Dong and coworkers [30] reported the elaboration of a nanocomposite of GNPs and porphyrin by depositing anionic $AuCl_4^-$ and cationic cobalt porphyrin onto an ITO substrate followed by electrochemical reduction. In previous work, we designed a series of porphyrin-functionalized carbon nano-

* Corresponding authors. Tel.: +86 25 83593593; fax: +86 25 83593593.
E-mail addresses: jpl@nju.edu.cn (J. Lei), hxju@nju.edu.cn (H. Ju).

0013-4686/$ – see front matter © 2011 Elsevier Ltd. All rights reserved.
doi:10.1016/j.electacta.2011.01.060

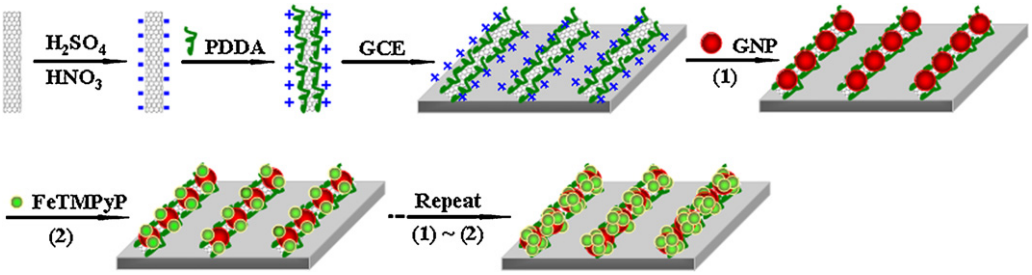

Scheme 1. Assembly process of FeTMPyP–GNPs on the PDDA-CNT-modified GCE.

materials and developed several electrocatalytic methods for the detection of biological molecules, such as trichloroacetic acid [31], chloramphenicol [32], sulfite [33], and chlorite [34].

Here, the FeTMPyP-functionalized GNPs assembled on PDDA-CNTs via electrostatic interactions showed well-defined redox peaks of Fe(III)TMPyP/Fe(II)TMPyP. The GNPs accelerated the electron transfer between FeTMPyP and the electrode, and the PDDA-CNTs insured the immobilization of the functionalized GNPs on the electrode surface. The modified electrode showed a high overpotential for the reduction of hydrogen peroxide and a sensitive response to PAA reduction because of the excellent electrocatalytic activity of FeTMPyP-functionalized GNPs, leading to a highly selective amperometric biosensor for PAA. This biosensor was successfully applied in the amperometric detection of PAA in a disinfectant sample and could provide a novel biosensing tool for environmental monitoring.

2. Experimental

2.1. Materials and reagents

FeTMPyP was a gift from Kanazawa University (Japan). Chloroauric acid ($HAuCl_4{\cdot}4H_2O$) and trisodium citrate were obtained from Shanghai Reagent Company (Shanghai, China). Multiwalled carbon nanotubes (CNTs; CVD method, purity ≥98%, diameter 20–40 nm, and length 1–2 μm) were purchased from Nanoport Co. Ltd. (Shenzhen, China). PAA was purchased from the Tongzhi Trade, Limited, Company (Shanghai, China). Poly(diallyldimethylammonium chloride) (PDDA; 20%, w/w in water, MW: 200,000–350,000) was obtained from Sigma–Aldrich Chemical Co. (St. Louis, MO). Phosphate-buffered saline (PBS, 0.1 M) solutions were prepared at various pH values by mixing stock solutions of NaH_2PO_4 and Na_2HPO_4. Ultrapure water obtained from a Millipore water-purification system (≥18 MΩ, Milli-Q, Millipore) was used in all assays. All other reagents were of analytical grade and used as received.

2.2. Apparatus

Electrochemical measurements were performed on a CHI 812B electrochemical analyzer (Co., CHI, USA) with a conventional three-electrode system. A glassy carbon electrode (GCE) (diameter 3 mm), a saturated calomel electrode (SCE), and a Pt electrode were used as the working electrode, reference electrode, and an auxiliary electrode, respectively. Scanning electron micrographs (SEMs) were obtained with a Hitachi S-3000N scanning electron microscope (Japan) at an acceleration voltage of 10 kV. The UV–vis spectra were measured with a UV-3600 UV–vis spectrophotometer (Shimadzu, Japan).

2.3. Fabrication of the biosensors

Colloidal GNPs 15 nm in diameter were prepared by quickly adding 2.5 mL 1% trisodium citrate to 100 mL of a boiling 0.01% $HAuCl_4$ solution and stirring the solution until deep red [35]. The PDDA-CNT composite was synthesized as described in our previous work [36]. The CNTs were first treated with 3:1 H_2SO_4/HNO_3 under sonication for 4 h to shorten the CNTs, remove metallic and carbonaceous impurities, and generate carboxylate groups on the CNT surfaces. Next, 0.5 mg mL^{-1} of the carboxylated CNTs was dispersed into a 0.20% PDDA aqueous solution containing 0.5 M NaCl by sonication for 30 min to give a homogeneous black suspension. After washing with water, the composite was dispersed into water to yield 0.5 mg mL^{-1} PDDA-CNTs.

The fabrication procedure for the biosensors is shown in Scheme 1. Prior to modification, the GCE was successively polished to a mirror finish using 1.0- and 0.05-μm alumina slurry (Beuhler). After successive sonication in ethanol and double-distilled water, the electrode was rinsed with double-distilled water and allowed to dry at room temperature. After casting 3 μL of PDDA-CNT (0.5 mg mL^{-1}) onto the surface, 4 μL of GNPs was dropped onto the electrode. After removing the unadsorbed GNPs, a negatively charged surface was formed for the assembly of 4 μL of FeTMPyP (400 μM). Afterwards, another layer of FeTMPyP–GNPs was assembled on the first layer of FeTMPyP–GNPs by the same casting of GNPs and FeTMPyP. In this way, the multilayer FeTMPyP–GNP coating was obtained.

3. Results and discussion

3.1. Characterization of FeTMPyP–GNP assembly

Because of their high surface-to-volume ratio and excellent conductivity, CNTs have been extensively investigated as essential carriers in the constructing of electrochemical biosensors by wrapping cationic PDDA on the sidewall surface of the carboxylated CNTs to facilitate loading the negatively charged materials. Fig. 1 shows SEM images of the CNTs, PDDA-CNTs, GNPs/PDDA-CNTs and $(FeTMPyP–GNPs)_2$/PDDA-CNTs on ITO substrates. The carboxylated CNTs obtained by chemical oxidation exhibited a homogeneous and even dispersion, with a diameter of around 30 nm (Fig. 1A). After wrapping with PDDA, the diameter of the CNTs did not show an obvious change (Fig. 1B). After assembly of the negatively charged GNPs, densely packed GNPs were observed on the surface of the PDDA-CNTs, with a slight increase in size (Fig. 1C). After two layers of FeTMPyP–GNPs were assembled, a more densely packed morphology was observed, as in Fig. 1D.

To further identify the interaction between GNPs and FeTMPyP, the UV–vis spectra of FeTMPyP, GNPs and FeTMPyP–GNPs were examined (Fig. 2). The characteristic absorption peaks of FeTMPyP and GNPs were at 422 nm and 519 nm, which corresponded to the Soret band of FeTMPyP and the plasmon band of GNPs, respec-

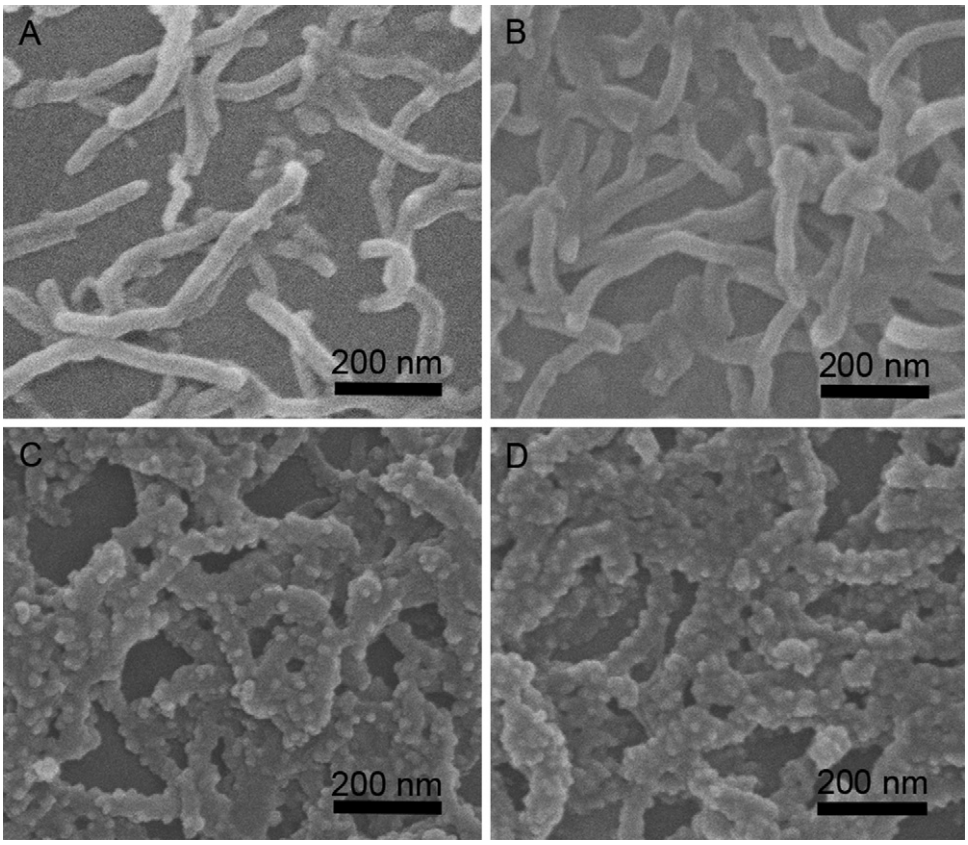

Fig. 1. SEM images of (A) CNTs, (B) PDDA-CNTs, (C) GNPs/PDDA-CNTs and (D) $(FeTMPyP–GNPs)_2$/PDDA-CNTs.

tively. In contrast, FeTMPyP–GNPs exhibited an absorption peak at 452 nm, differing from the characteristic peaks of both FeTMPyP and GNPs. The red shift of FeTMPyP at the Soret band could be considered to be a consequence of the aggregation effects resulting from the GNPs [37].

3.2. Electrochemical behavior of $(FeTMPyP–GNPs)_2$/PDDA-CNT-modified GCE

The cyclic voltammogram of GNPs/PDDA-CNT-modified GCE in N_2-saturated PBS did not show an observable peak in the potential range of −0.9 V to 0.4 V (Fig. 3A, curve a), whereas the $(FeTMPyP–GNPs)_2$/PDDA-CNT-modified GCE showed stable and well-defined redox peaks at −0.112 V and −0.154 V (Fig. 3A, curve b), which were attributed to the redox couple Fe(III)TMPyP/Fe(II)TMPyP. Compared with the single layer of FeTMPyP–GNPs (Fig. 3A, curve c), the reduction peak current of $(FeTMPyP–GNPs)_2$/PDDA-CNT-modified GCE increased from 1.82 μA to 2.32 μA. The peak-to-peak separation of 0.042 V was smaller than the 0.058 V reported for a tetraphenylporphyrin/CNT-modified electrode [38], indicating a higher electron-transfer rate. From the peak area, the amount of FeTMPyP immobilized on the $(FeTMPyP–GNPs)_2$/PDDA-CNT-modified GCE was calculated at 6.18×10^{-10} mol cm^{-2}, which was much larger than the monolayer coverage and that of the 3.80×10^{-11} mol cm^{-2} reported for cobalt tetramethoxyphenyl porphyrin on GCE [39], and could be attributable to the larger apparent area because of the presence of both GNPs and PDDA-CNTs.

The reduction and oxidation peak currents of the $(FeTMPyP–GNPs)_2$/PDDA-CNT-modified GCE in 0.1 M N_2-saturated PBS increased linearly with increasing scan rate from 25 to 500 mV s^{-1} (Fig. 3B), indicating a surface-controlled process. With

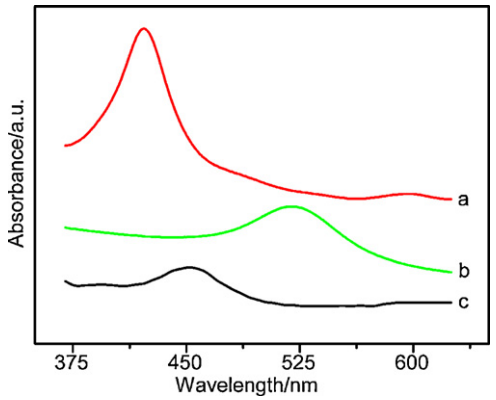

Fig. 2. UV–vis spectra of (a) FeTMPyP, (b) GNPs and (c) FeTMPyP–GNPs.

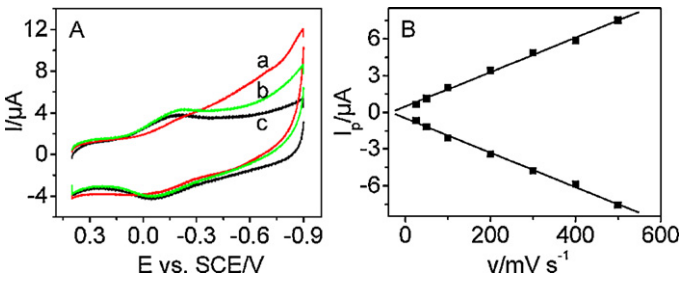

Fig. 3. Cyclic voltammograms (A) of (a) GNPs/PDDA-CNT-, (b) $(FeTMPyP–GNPs)_2$/PDDA-CNT- and (c) FeTMPyP–GNPs/PDDA-CNT-modified GCEs in N_2-saturated PBS at 100 mV s^{-1} and plots of oxidation and reduction peak currents of $(FeTMPyP–GNPs)_2$/PDDA-CNT-modified GCE *vs.* scan rate (B).

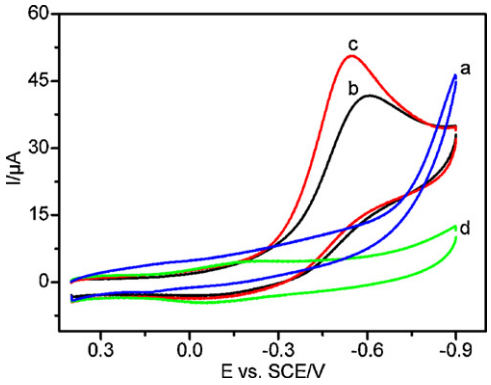

Fig. 4. Cyclic voltammograms of (a) GNPs/PDDA-CNT- and (b) FeTMPyP–GNPs/PDDA-CNT-modified GCE in N_2-saturated PBS containing 200 μM PAA, and (FeTMPyP–GNPs)$_2$/PDDA-CNTs modified GCE in N_2-saturated PBS containing 200 μM PAA (c) and H_2O_2 (d). Scan rate: 100 mV s^{-1}.

increasing pH from 5 to 8, the reduction potential shifted linearly to more negative values, with a slope of −56.3 mV pH^{-1}, which is closed to the theoretical value of −59.1 mV pH^{-1} at 25 °C for a one-proton/one-electron electrode process, indicating that one proton participated in the redox process.

3.3. Electrocatalytic reduction of PAA

Fig. 4 shows the electrocatalytic response of PAA at GNPs/PDDA-CNT-, FeTMPyP–GNPs/PDDA-CNT- and (FeTMPyP–GNPs)$_2$/PDDA-CNT-modified GCEs in 0.1 M PBS. When 200 μM PAA was added to the solution, the GNPs/PDDA-CNT-modified GCE showed no response in the potential range from −0.9 V to 0.4 V (Fig. 4a). However, both the FeTMPyP–GNPs/PDDA-CNT- and (FeTMPyP–GNPs)$_2$/PDDA-CNT-modified GCEs showed sensitive electrocatalytic responses to PAA at −0.593 V and −0.543 V, respectively (Fig. 4b and c), which suggests that FeTMPyP had an electrocatalytic activity for the reduction of PAA. The slight positive shift of peak potential was attributed to the more densely packed GNPs on the PDDA-CNTs, which accelerated the electron transfer between FeTMPyP and the electrode. A possible mechanism is that Fe(III)TMPyP is first reduced to Fe(II)TMPyP at the electrode surface followed by binding with PAA to form a ferrous-peroxo intermediate [11,40] and, at a more negative potential, the complex is further reduced to give the product and release Fe(II)TMPyP. The slightly more positive reduction potential and higher reduction peak current of PAA at the (FeTMPyP–GNPs)$_2$/PDDA-CNT-modified GCE than with the FeTMPyP–GNPs/PDDA-CNTs resulted from the increased amount of FeTMPyP, improving the catalytic ability. Interestingly, when 200 μM H_2O_2 was added to the solution, the cyclic voltammogram of the (FeTMPyP–GNPs)$_2$/PDDA-CNT-modified GCE showed no change (Fig. 4d), indicating a high overpotential for the reduction of H_2O_2 at the modified electrode. Although Fe(II)TMPyP can also form a peroxo complex with hydrogen peroxide, both the poor ligating power of HOOH and more difficult O–O bond heterolysis resulted in a slower kinetic process for H_2O_2 catalytic reduction on iron porphyrins in an aqueous medium [40]. This behavior provided an advantage for construction of a PAA biosensor for use in cosolution with H_2O_2.

3.4. Optimization of biosensor fabrication

The effect of the amount of PDDA-CNTs on the electrocatalytic response of the biosensor to 200 μM PAA is shown in Fig. 5A. When the volume of PDDA-CNT was increased from 1 μL to 5 μL, the electrocatalytic response increased and trended to a stable response at the amount of 3 μL. Therefore, 3 μL of PDDA-CNTs

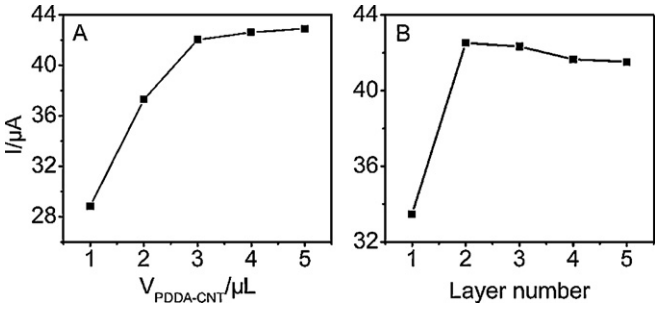

Fig. 5. Effects of (A) the amount of PDDA-CNTs and (B) layer number of FeTMPyP–GNPs used for the preparation of the biosensor on the electrocatalytic response to 200 μM PAA.

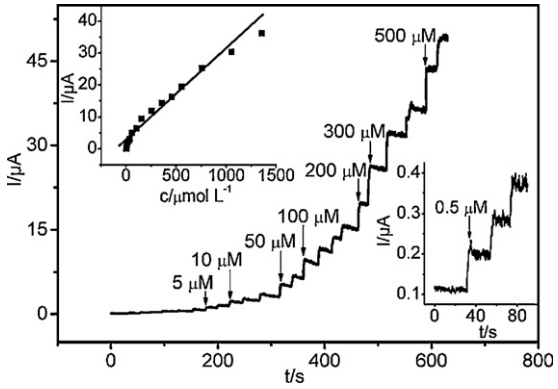

Fig. 6. Typical current–time response curve of the biosensor upon successive additions of PAA at an applied potential of −0.55 V. Upper inset: linear calibration curve. Lower inset: amplified response curve.

was determined to be the optimal applied volume. The layer number of FeTMPyP–GNPs also affected the electrocatalytic response (Fig. 5B). When the layer number was increased from one to five, the electrocatalytic response increased, showing a maximum value at two layers. The decreased response at higher layer numbers was attributed to the decrease in both the accessibility to catalytic sites for PAA reduction and the electron-transfer rate. Thus, subsequent work used two layers of FeTMPyP/GNPs to prepare the PAA biosensor.

3.5. Amperometric sensing of PAA

The steady-state amperometric responses of the biosensor to different amounts of PAA were determined at −0.55 V by successive addition of PAA into 6 mL of PBS. Upon the addition of PAA, the response immediately increased and reached 95.3% of the steady-state current within 3 s (Fig. 6). The linear range spanned three orders of magnitude, from 2.5×10^{-6} to 1.05×10^{-3} M. The detection limit at a signal-to-noise ratio of 3 was 0.5 μM. The linear response range was wider than that reported for a rotating Au electrode (0.36–110 mM) [9], and the detection limit was lower (0.22 mM) [10].

The stability and repeatability of the PAA biosensor were evaluated. The responses to six successive additions of 0.05 mM PAA showed a relative standard deviation (RSD) of 4.2%, demonstrating a good repeatability. The RSD of current signals for the measurement of 0.05 mM PAA with six independently prepared biosensors was 3.1%, demonstrating the good fabrication reproducibility of the biosensor. When stored in air and measured at intervals of two days, the sensor still retained 95.8% of the initial response after two weeks. This implies that the structure of (FeTMPyP–GNPs)$_2$/PDDA-CNTs is very efficient for retaining the activity of FeTMPyP and

preventing it from leaking out of the biosensor. The average recovery of the method for the detection of PAA in a disinfectant sample was ~98.6 ± 3.37% (n = 3), suggesting an acceptable stability of the biosensor in practical applications.

4. Conclusions

Porphyrin-functionalized GNPs were successfully assembled onto a PDDA-CNT-modified electrode via a layer-by-layer technique. GNPs were densely packed on the PDDA-CNTs, improving the electrochemical response. Moreover, because of the strong electrostatic interactions, the electronic communication in the ground state between FeTMPyP and the GNPs was realized, leading to an accelerated electron transfer and the development of an efficient biosensor. Based on the efficient electrocatalysis of the iron porphyrin, the first biosensor was constructed for the selective detection of PAA in the presence of H_2O_2 and showed a good performance with a rapid response, a wide linear range, a low detection limit and good fabrication reproducibility. The functionalization of gold nanoparticles with the porphyrin provided a facile way of preparing ordered biofunctional materials for use as a specific and efficient electrochemical transducer in biosensing.

Acknowledgements

This work was financially supported by the National Basic Research Program of China (2010CB732400), the National Natural Science Foundation of China (20705012, 20875044, 20821063, 21075060), and the Ph.D. Fund for Young Teachers (20070284052).

References

[1] U. Pinkernell, U. Karst, K. Cammann, Anal. Chem. 66 (1994) 2599.
[2] M.I. Awad, T. Oritani, T. Ohsaka, Anal. Chem. 75 (2003) 2688.
[3] M.M. Samrakandi, C. Roques, G. Michel, Pathol. Biol. 42 (1994) 432.
[4] N. Higashi, H. Yokota, S. Hiraki, Y. Ozaki, Anal. Chem. 77 (2005) 2272.
[5] S. Effkemann, U. Pinkernell, R. Neumüller, F. Schwan, H. Engelhardt, U. Karst, Anal. Chem. 70 (1998) 3857.
[6] B.N. Ferdousi, M.M. Islam, T. Okajima, T. Ohsaka, Talanta 74 (2008) 1355.
[7] M. Onoda, S. Uchiyama, T. Santa, K. Imai, Anal. Chem. 74 (2002) 4089.
[8] M. Pacenti, S. Dugheri, P. Boccalon, G. Arcangeli, P. Dolara, V. Cupelli, Ind. Health 48 (2010) 217.
[9] M.I. Awad, C. Harnoode, K. Tokuda, T. Ohsaka, Anal. Chem. 73 (2001) 1839.
[10] R. Toniolo, A. Pizzariello, S. Susmel, N. Dossi, G. Bontempelli, Electroanalysis 18 (2006) 2079.
[11] J.P. Collman, R. Boulatov, C.J. Sunderland, L. Fu, Chem. Rev. 104 (2004) 561.
[12] J. Heinecke, P.C. Ford, Coord. Chem. Rev. 254 (2010) 235.
[13] C. Pichon-Santander, P.J. Santander, A.I. Scott, Bioorg. Med. Chem. 14 (2006) 3904.
[14] M. Kunieda, H. Tamiaki, J. Org. Chem. 73 (2008) 7686.
[15] T. Yamaguchi, K. Tsukamoto, O. Ikeda, R. Tanaka, T. Kuwabara, K. Takahashi, Electrochim. Acta 55 (2010) 6042.
[16] F. Charreteur, F. Jaouen, J.P. Dodelet, Electrochim. Acta 54 (2009) 6622.
[17] W.M. Ching, C.H. Chuang, C.W. Wu, C.H. Peng, C.H. Hung, J. Am. Chem. Soc. 131 (2009) 7952.
[18] L.E. Goodrich, F. Paulat, V.K.K. Praneeth, N. Lehnert, Inorg. Chem. 49 (2010) 6293.
[19] T.C. Berto, V.K.K. Praneeth, L.E. Goodrich, N. Lehnert, J. Am. Chem. Soc. 131 (2009) 17116.
[20] X.Q. Lu, F.P. Zhi, H. Shang, X.Y. Wang, Z.H. Xue, Electrochim. Acta 55 (2010) 3634.
[21] A. Okunola, B. Kowalewska, M. Bron, P.J. Kulesza, W. Schuhmann, Electrochim. Acta 54 (2009) 1954.
[22] Z.B. Liu, Y.F. Xu, X.Y. Zhang, X.L. Zhang, Y.S. Chen, J.G. Tian, J. Phys. Chem. B 113 (2009) 9681.
[23] J.X. Geng, H.T. Jung, J. Phys. Chem. C 114 (2010) 8227.
[24] W.M. Campbell, A.K. Burrell, D.L. Officer, K.W. Jolley, Coord. Chem. Rev. 248 (2004) 1363.
[25] S.O. Obare, T. Ito, G.J. Meyer, J. Am. Chem. Soc. 128 (2006) 712.
[26] G.F. Moore, M. Hambourger, M. Gervaldo, O.G. Poluektov, T. Rajh, D. Gust, T.A. Moore, A.L. Moore, J. Am. Chem. Soc. 130 (2008) 10466.
[27] Y.X. Xu, L. Zhao, H. Bai, W.J. Hong, C. Li, G.Q. Shi, J. Am. Chem. Soc. 131 (2009) 13490.
[28] A.J. Morris, G.J. Meyer, E. Fujita, Acc. Chem. Res. 42 (2009) 1983.
[29] E. Maligaspe, A.S.D. Sandanayaka, T. Hasobe, O. Ito, F. D'Souza, J. Am. Chem. Soc. 132 (2010) 8158.
[30] M.H. Huang, Y. Shen, W.L. Cheng, Y. Shao, X.P. Sun, B.F. Liu, S.J. Dong, Anal. Chim. Acta 535 (2005) 15.
[31] W.W. Tu, J.P. Lei, H.X. Ju, Chem. Eur. J. 15 (2009) 779.
[32] W.W. Tu, J.P. Lei, L. Ding, H.X. Ju, Chem. Commun. 28 (2009) 4227.
[33] W.W. Tu, J.P. Lei, G.Q. Jian, Z. Hu, H.X. Ju, Chem. Eur. J. 16 (2010) 4120.
[34] W.W. Tu, J.P. Lei, S.Y. Zhang, H.X. Ju, Chem. Eur. J. 16 (2010) 10771.
[35] A. Ambrosi, M.T. Castaneda, A.J. Killard, M.R. Smyth, S. Alegret, A. Merkoci, Anal. Chem. 79 (2007) 5232.
[36] G.S. Lai, F. Yan, H.X. Ju, Anal. Chem. 81 (2009) 9730.
[37] A. Kotiaho, R. Lahtinen, H. Lehtivuori, N.V. Tkachenko, H. Lemmetyinen, J. Phys. Chem. C 112 (2008) 10316.
[38] Q. Zhao, Z.N. Gu, Q.K. Zhuang, Electrochem. Commun. 6 (2004) 83.
[39] H.S. Liu, L. Zhang, J.J. Zhang, D. Ghosh, J. Jung, B.W. Downing, E. Whittemore, J. Power Sources 161 (2006) 743.
[40] J.P. Collman, M. Kaplun, C.J. Sunderland, R. Boulatov, J. Am. Chem. Soc. 126 (2004) 11166.